JOURNAL OF MECHANICAL ENGINEERING AND SCIENCES
ISSN: 2289-4659 e-ISSN: 2231-8380
VOLUME 19, ISSUE 1, 2025, 10493 - 10507
DOI: https://doi.org/10.15282/jmes.19.1.2025.5.0822

UNIVERSITI MALAYSIA PAHANG AL-SULTAN ABDULLAH

RESEARCH ARTICLE

Optimization of maskless electrochemical microtexturing

S. Kunar

Department of Mechanical Engineering, Aditya University, Surampalem 533437, India
Phone: +91- 8420298463

ABSTRACT - Surface microtexturing method is utilized to improve the vital functions in various engineering disciplines like tribological, biocompatibility, and sustainability. The generation of microtexturing is difficulty by other advanced micromachining methods such as heat affecected zone in laser micromachining and micro electric discharge machining, and low production efficiency in abrasive jet micromachining. The microtexturing with micro circular pattern, generated using maskless electrochemical microtexturing in indigenously developed experimental setup is investigated. The developed setup consists of experimental cell, power connections and electrolyte flow system. The SU-8 2150 insulated textured tool is more advantageous for producing microstructures. Hence, it was reused many times for microtextured production. The influence of various process parameters like voltage, duty ratio, frequency, inter electrode gap (IEG), flow rate and machining time on numerous important microtexturing characteristics such as material removal rate (MRR) overcut, depth and surface roughness is investigated. Furthermore, a new and efficient method i.e. evaluation based on distance from average solution (EDAS) was used to identify the optimal combination of microtexturing process parameters. The achieved optimal parameters are voltage of 10 V, duty ratio of 40%, frequency of 5 kHz, IEG of 100 µm, flow rate of 5 m^3/h and machining time of 5 minutes for manufacturing of accurate micropatterns. From the confirmation experiments using EDAS, the best machined characteristics are MRR of 5.2 mg/min, overcut of 25.41 µm, depth of 8.2 µm and surface roughness, R_a of 0.0278 µm.

ARTICLE HISTORY
Received : 26th June 2024
Revised : 04th Dec. 2024
Accepted : 24th Feb. 2025
Published : 30th Mar. 2025

KEYWORDS
Electrochemical microtexturing
Micro circular pattern
EDAS
Machining characteristics

1. INTRODUCTION

Generation of micro-texturing is a prospective approach for the application of micro engineering parts. Scientists and engineers worldwide have intentionally designed and produced different micro-textures to enhance the performance of various components. These performances usually comprise the extreme wettability [1], biocompatibility of medical implants [2] and others. Different processes have been developed for forming surface microstructures, such as ultrasonic vibration machining [3], abrasive jet machining [4], chemical etching [5], maskless electrochemical micromachining (EMM) [6], and laser beam machining [7]. Textured surfaces serve as reservoirs of fluid and between mating components retain the lubricating thin film. Textured surface retains the lubrication in mating surfaces for reducing the friction in mechanical components. In addition, contemporary progress has been demonstrated in the fields of optics, aerospace, automotive, aviation, miniature manufacturing, etc. and micro circular patterns have been successfully generated in difficult to machine materials. Amongst all the micromanufacturing techniques, maskless EMM has lots of advantages such as, no thermal damage and formation of residual stresses on processed surface and no change in mechanical properties of job material [8]. So, it is more prominent technique for producing micro-textures. Maskless electrochemical microtexturing is used to apply in biomedical applications, optical components and devices, microfluidics and lab-on-a-chip, semiconductor industry, etc.

To compute the outcome of process parameters and to present the impact of process variables during the generation of dimple patterns, a mathematical model is used [9]. Optimizing process parameters are crucial for the insight of higher production, which is the opening source for endurance in today's economical market conditions. Combined regulation of various process parameters will achieve the optimum output of electrochemical machining workpieces [10]. For the optimization of machining parameters during drilling of AI/SiC metal matrix composite [11], the application of Grey relational analysis and analysis of variance is used. The foamed cathode through mask EMM is modified as sandwich-like structure using magnetic field force for conducting the experiments to obtain the best machining results [12]. This modified setup is not proficient for generating the micro-textures because the electrolytic products may accumulate in the narrow machining zone results in deterioration of machining accuracy. The optimization of air shielding electrochemical micromachining including nozzle inclination and process parameters are studied using grey relational analysis method for generation of microstructures [13]. The investigation is conducted utilizing of SKD 11 tool steel workpiece and brass electrode using the L9 orthogonal array [14]. The porous and flexible electrode is used for micro texturing on any curved surface using through-mask electrochemical micromachining [15]. Methods of multi-response optimization such as technique for order preference by similarity to ideal solution (TOPSIS) and Victoria method (VIKOR) are used to optimize the different parameters for micro-feature manufacturing [16]. The influence and parametric optimization of

*CORRESPONDING AUTHOR | S. Kunar | ✉ sandipkunar@adityauniversity.in

process variables are investigated for EMM using Grey relational analysis method. The experimental results demonstrate that conical electrodes with rounded form electrodes are used for the generation of micro characteristics [17]. A recent multi-criteria decision-making (MCDM) approach, the Evaluation Based on Distance from Average Solution, is suitable for solving various complex real-world problems associated with decision-making, especially those related to ambiguity [18]. However, the availability of literature on the application of EDAS technique in solving machining problems is precisely limited if at all. The EDAS method is used because Evaluating based on the distance from an average solution provides a way to assess how much a given solution deviates from the norm, helping to track progress, balance exploration with exploitation, avoid local optima, and monitor convergence. This technique makes it easier to measure the quality of solutions, adjust the optimization process dynamically, and ensure that the search space is adequately explored.

The most efficient process i.e., EDAS method is presented using different electrochemical microtexturing process variables to explore the influences during generation of micro circular pattern. This research shows that this technique is relatively applicable to the production of micropatterns on SS-304 using the established setup and flow method. One textured tool can generate multiple machined samples. Influence and parametric optimization of process parameters such as IEG, duty ratio, machining time, voltage, frequency, and flow rate are investigated using the EDAS method on machining characteristics i.e., depth, surface roughness, R_a, overcut and material removal rate. To find out the significant process inputs for producing the dimple pattern, this optimization technique is used. The confirmation experiment is also conducted using the optimized parameter setting and micrograph-based analysis has then been performed.

2. MATERIALS AND METHODS

To produce micro circular pattern as shown in Figure 1, the experimental setup is indigenously designed. It requires experimental cell, fixtures for electrodes, electrical connection, and electrolyte circulation system. Material from Perspex is used to manufacture fixtures for experimental cell and electrodes. The cell outlet and inlet ports are manufactured using stainless steel. The vertical cross flow electrolyte method is mainly the significant feature, integrated within the formed experimental cell. The created additional back pressure is produced for this feature, which removes the sludge from the narrow micromachining region. This flow improves micro-textures' machining precision and surface quality. The pulsed direct current power supply supplies the power link. The cell with electrode fixtures is shown in Figure 2. For the development of tool with a diameter of 193 µm on stainless sheet using the SU-8 2150 mask, a ultraviolet exposure device is used. The thickness of textured mask is 205 µm.

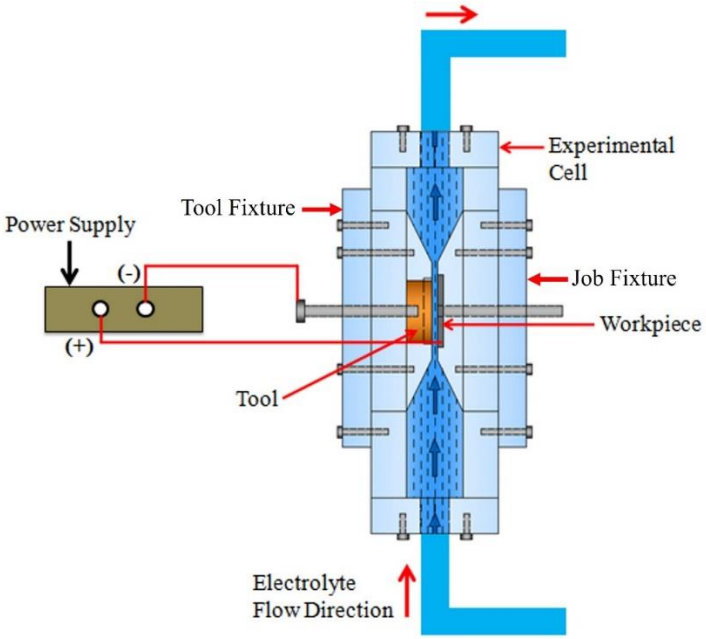

Figure 1. Experimental setup

The essential processing parameters for manufacture of required micro-textures are determined for good industrial use of this setup. Impacting parameters on the textured features namely machining depth, MRR, surface roughness and overcut, are explored, such as flow rate, machining time, voltage, duty ratio, IEG and frequency on SS 304 workpiece. To investigate the effect of different parameters using maskless electrochemical microtexturing method, the most influencing EMM process parameters are decided on the basis of literature and lot of trial experiments for experimental investigations. The effect of major EMM parameters on machined characteristics of microtextures is investigated by varying one variable at a time keeping other parameters constant.The ranges are 2 to 5 m^3/h, 100 to 250 µm, 8 to 14 V, 20 to 50%, 3 to 6 kHz, and 2 to 5 min respectively for flow rate, IEG, voltage, duty ratio, frequency, and machining time. The $NaNO_3$ (50%) and NaCl (50%) mixed electrolyte concentration is 20 g/l. With an optical microscope and a three dimensional (3D) non-contact profilometer, the textured responses are measured.

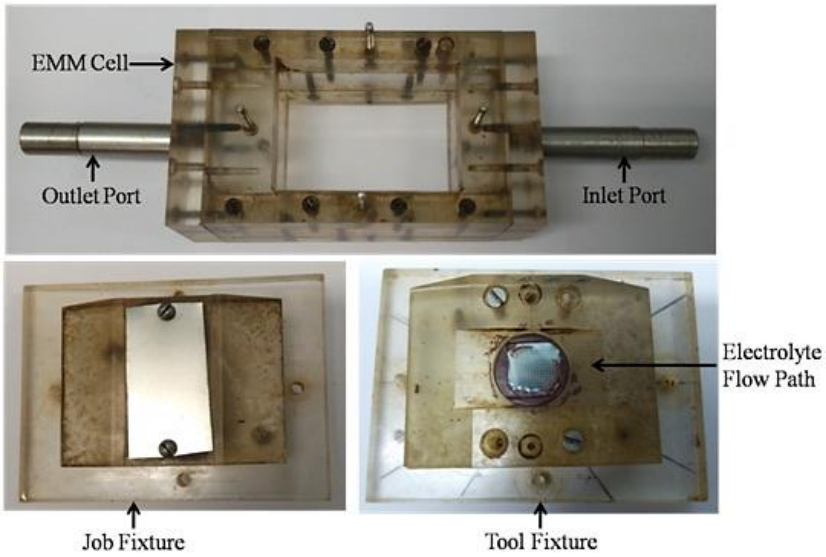

Figure 2. Developed cell with electrodes holding device

3. RESULTS AND DISCUSSION

Investigation is conducted to represent the outcome of input parameters on micro-structured characteristics during micropattern formation and to evaluate the most important parametric combination using the unique method of efficient and effective optimization of EDAS. The confirmation experiments and micrograph analysis are performed after obtaining this setting. The overcut is changed due to stray current effect in the output parameters [8]. The experimental results are represented in Table 1.

Table 1. Machining response

Sl. No.	Input Parameters						Output Parameters			
	Voltage (V)	Duty ratio (%)	Frequency (kHz)	Inter Electrode Gap (μm)	Flow Rate (m^3/h)	Time (min)	MRR (mg/min)	Overcut (μm)	Depth (μm)	R_a (μm)
1	8	20	6	100	5	2	4.8	28.125	7.10	0.0379
2	10	20	6	100	5	2	5.7	41.200	8.74	0.0718
3	12	20	6	100	5	2	6.9	47.325	12.2	0.1660
4	14	20	6	100	5	2	7.5	53.321	28.2	0.2470
5	8	20	6	100	5	2	4.8	28.120	7.10	0.0379
6	8	30	6	100	5	2	6.1	36.810	8.77	0.0607
7	8	40	6	100	5	2	6.7	42.220	10.50	0.1240
8	8	50	6	100	5	2	8.4	53.230	21.80	0.2480
9	8	20	3	100	5	2	8.3	59.284	25.80	0.2680
10	8	20	4	100	5	2	8.2	47.012	23.30	0.2480
11	8	20	5	100	5	2	7.9	39.049	11.60	0.0713
12	8	20	6	100	5	2	4.8	28.125	7.10	0.0379
13	8	20	6	100	5	2	4.8	28.125	7.10	0.0379
14	8	20	6	150	5	2	4.4	39.464	6.50	0.0558
15	8	20	6	200	5	2	2.9	51.158	6.1	0.0684
16	8	20	6	250	5	2	1.1	57.731	5.2	0.0695
17	8	20	6	100	2	2	1.6	54.285	5.1	0.5260
18	8	20	6	100	3	2	3.1	42.826	6.1	0.3810
19	8	20	6	100	4	2	3.8	39.235	6.5	0.1650
20	8	20	6	100	5	2	4.8	28.125	7.1	0.0379
21	8	20	6	100	5	2	4.8	28.125	7.1	0.0379
22	8	20	6	100	5	3	5.4	41.866	14.4	0.0537
23	8	20	6	100	5	4	5.8	46.274	15.1	0.0586
24	8	20	6	100	5	5	7.8	57.862	18.1	0.0593

3.1 Influence of Process Variables on Microtextured Characteristics

The impact of voltage on MRR, surface roughness, overcut, and machining depth is revealed in Figure 3. With increasing voltage, the electrical conductivity increases with greater voltage resulting in greater material removal. The overcut enlarges with boosting voltage caused by a higher stray current effect. With increasing voltage, the machining depth increases due to controlled machining across the microtextures. The surface roughness rises owing to uneven etching with higher voltage.

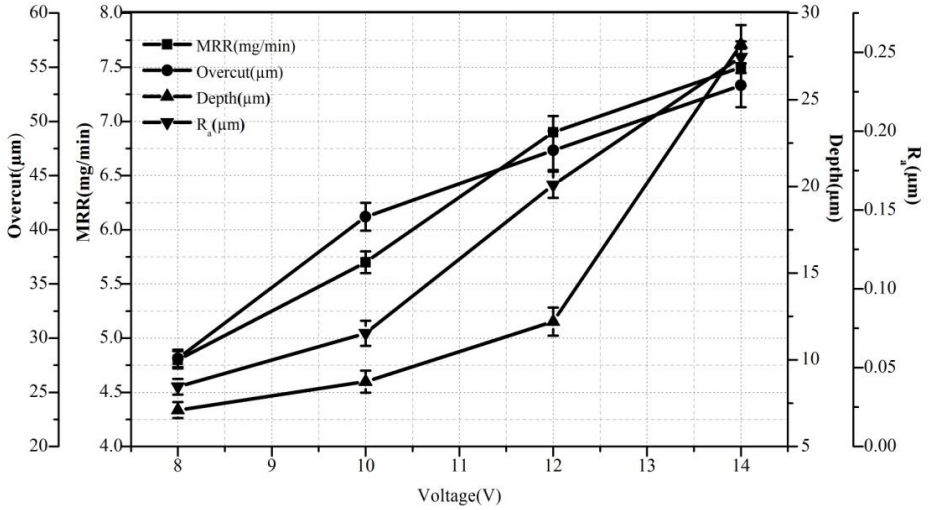

Figure 3. MRR, overcut, depth and R_a variation with voltage

As shown in Figure 4, experiments are conducted to investigate the outcome of duty ratio on MRR, depth, overcut, and surface roughness. With incresing the duty ratio, the machining time increases resulting in higher MRR from the microtextures. The stray current effect increases because the the machining time rises in higher duty ratio resulting in the higher overcut. Because of controlled machining for more machining time in higher duty ratio, the machining depth increases. The surface roughness rises due to rough machining with a higher duty ratio for the availability of higher pulse on time.

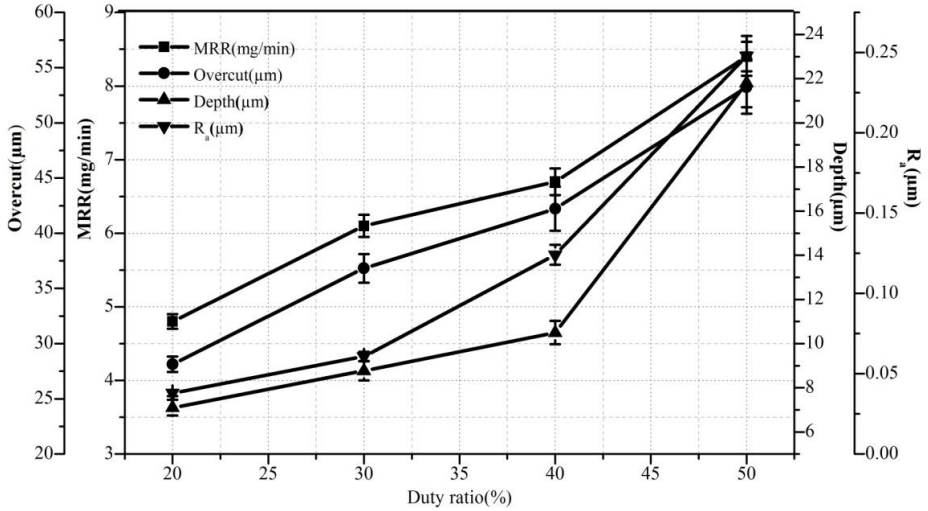

Figure 4. MRR, overcut, depth and R_a variation with duty ratio

From Figure 5, the variance of MRR, depth, overcut and surface roughness is shown with changing of frequency. The MRR drops off with greater frequency owing to lower repetition of pulse on time. With rising frequency, the overcut decreases due to lower stray current effect for less pulse on time. Due to less localization of machining, the depth diminishes with rising frequency. With rising frequency, the surface roughness often drops off due to regular etching for reduced machining time.

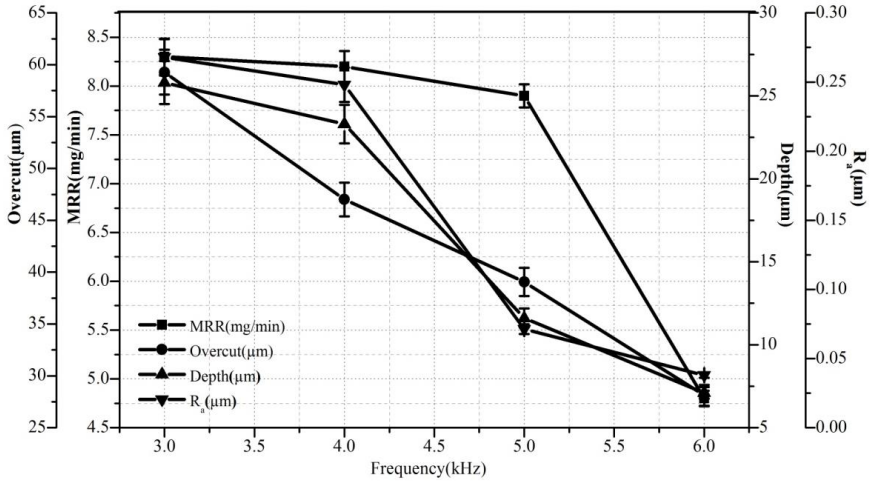

Figure 5. MRR, overcut, depth and R_a variation with frequency

The variant of IEG explores the dissimilarity of surface roughness, MRR, overcut and depth. From Figure 6, MRR decreases because of higher ohmic resistance with rising IEG. Because of irregular distribution of current density, the overcut enlarges with growing IEG. Due to less localization of machining with increasing IEG, the depth decreases. As the IEG augments, the surface roughness increases by reason of irregular etching.

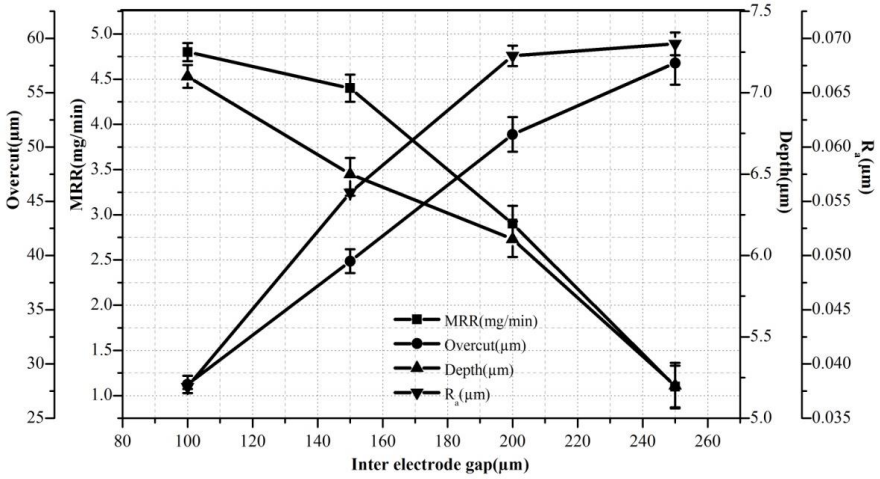

Figure 6. MRR, overcut, depth and R_a variation with IEG

In Figure 7, the variance of surface roughness, MRR, depth and overcut is shown with the change of flow rate. As the flow rate increases, the MRR increases due to greater current density. Owing to the removal of electrolysis products with lower stray current effect, the overcut declines with rising flow rate. Due to further localization of machining, the machining depth increases with higher flow rate. The surface roughness reduces due to consistent etching across the micromachining region with greater flow rate.

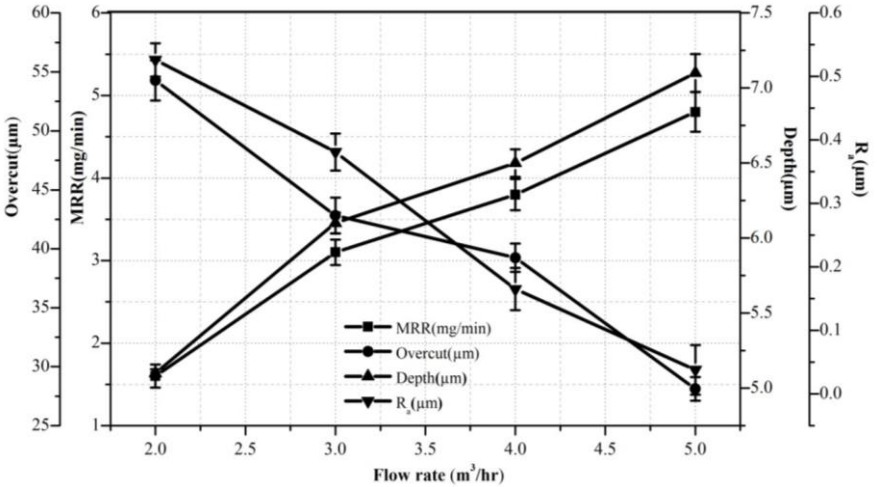

Figure 7. MRR, overcut, depth and R_a variation with flow rate

The outcome of machining time on depth, MRR, surface roughness and overcut is characterized in Figure 8. Due to more regulated machining for longer machining time, the MRR increases. Due to elevated stray current effect for larger machining time, the overcut rises. Due to superior machining localization, the depth raises with higher machining time. The surface roughness rises due to inhomogeneous current density distribution across the microtextures and rough machining takes place throughout the micropattern.

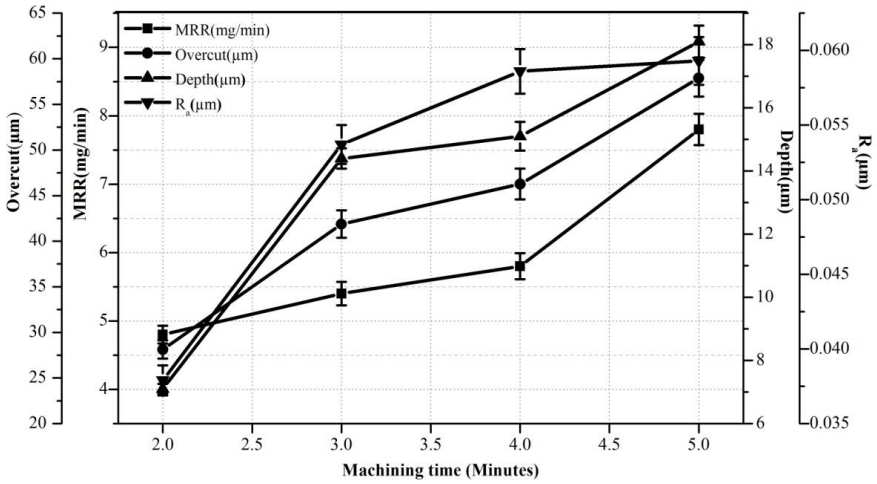

Figure 8. MRR, overcut, depth and R_a variation with machining time

The masked tool has more strength for producing multiple micropatterned samples. The environmental variations do not affect the Maskless electrochemical microtexturing method. One tool is reprocessed over eighteen times to conduct the experiments using the optimal parameters. It has no distortion during creation of several micropatterns. It is reclaimed lots of due to higher structural strength, higher resistance to tolerate higher flow rate, etc. These consequences recommend that this coating tool generate more machined micropatterns without distortion of mask.

3.2 Evaluation based on Distance from Average Solution

The EDAS method was developed by Ghorabaee, Zavadskas, Olfat and Turskis for multi-criteria inventory classification problems [19]. Based on two scales of negative distance from average (NDA) and positive distance from average (PDA), the authors ranked the materials. The desirability of the alternatives is correlated with both PDA and NDA measures and establishes the difference between average solution and each solution. The ranking of alternatives is based on higher values for PDA and lower values for NDA. When the PDA value is higher and/or the NDA value is lower, the outcome is considered better. The EDAS method compared with some of the current popular MCDM techniques such as VIKOR, TOPSIS, simple additive weighting and complex proportional assessment and reported the simplicity, stability and accuracy of EDAS method. Hence, this method can also be used successfully to solve MCDM problems.

The detailed procedure of the EDAS method is defined as follows [20, 21]:

- Step I: Selection of the most significant criteria defining the alternatives.
- Step II: Preparing the decision-making matrix, Z as seen below:

$$Z = [Z_{ab}]_{i\times j} \tag{1}$$

where, Z_{ab}represents the performance value of ath alternative on bth criterion.

- Step III: Determining average solution, A_b as per the criteria from Step I, using the following equation:

$$A_b = \frac{\sum_{a=1}^{i} Z_{ab}}{i} \tag{2}$$

- Step IV: Estimation of PDA using the following equations:

  If b^{th} criterion is beneficial,

$$PDA_{ab} = \frac{max(0,(Z_{ab} - A_b))}{A_b} \tag{3}$$

  If b^{th} criterion is non-beneficial,

$$PDA_{ab} = \frac{max(0,(A_b - Z_{ab}))}{A_b} \tag{4}$$

- Step V: Estimation of NDA, using the equations shown below:

If b^{th} criterion is beneficial,

$$NDA_{ab} = \frac{max(0,(A_b - Z_{ab}))}{A_b} \tag{5}$$

If b^{th} criterion is non-beneficial,

$$NDA_{ab} = \frac{max(0,(Z_{ab} - A_b))}{A_b} \tag{6}$$

- Step VI: Determination of the weighted sum of PDA using the following equation:

$$SP_a = \sum_{b=1}^{j} F_b PDA_{ab} \tag{7}$$

where, F_b is the relative fuzzy weight of bth criterion is calculated as follows:

$$F_b = \frac{F_{abs(s)}}{\sum_{b=1}^{k} F_{abs(s)}} \tag{8}$$

where, $F_{abs(s)} = \frac{1}{m}\sum_{j=1}^{m} FW_{avg(j)}$ is the absolute fuzzy weight where $1 \leq j \leq m$ and $1 \leq s \leq k$, $FW_{avg(j)} = \frac{1}{n}\sum_{i=1}^{n} FW_{(DM_i)}^{(j)}$ is the average fuzzy weight for each criterion, n is the number of decision maker and $FW_{(DM_i)}^{(j)}$ are average fuzzy weight corresponding to j.

- Step VII: Determination of the weighted sum of NDA using the following equation:

$$SN_a = \sum_{b=1}^{j} F_b NDA_{ab} \tag{9}$$

- Step VIII: Normalization of the values of SP and SN, using equations as follows:

$$NSP_a = \frac{SP_a}{max_a(SP_a)} \tag{10}$$

$$NSN_a = 1 - \frac{SN_a}{max_a(SN_a)} \tag{11}$$

- Step IX: Normalize the NSP and NSN values to determine Appraisal Score (AS) as shown below:

$$AS_a = \frac{1}{2}(NSP_a + NSN_a) \tag{12}$$

where, $0 \leq AS_a \leq 1$

- Step X: Alternatives are ordered in descending order of their AS.

The option with the maximum AS is perceived to be the best of the different alternatives.

3.2.1 Multi-objective optimization of EMM process using EDAS method

The EDAS method is one of the most appropriate and recent methods for solving multi-objective problems in the manufacturing environment. Therefore, to take advantage of this novel method, an attempt was made to determine the optimum process parametric setting in the current research investigation. Input parameters such as voltage, machining time, duty ratio, frequency, IEG, and flow rate are applied during micro-texturing of stainless steel to achieve full MRR & machining depth and minimum overcut & surface roughness. MRR and machining depth have been considered as beneficial criterion whereas overcut and surface roughness is non-beneficial criterion in the present research work. The model of input-process-output of EMM process is shown in Figure 9.

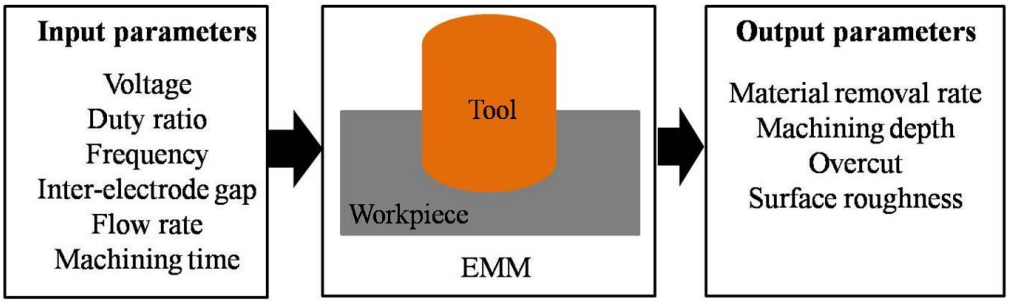

Figure 9. Input-process-output diagram of EMM process

Appropriate linguistic variables defined by triangular fuzzy numbers [21] in the range of [0;1] as presented in Table 2 have been assigned significant weights for the respective micro-texturing performance characteristics. The opinion of four experts was obtained during the decision-making process. The experts rated each machining performance attribute with a suitable weight based on their experience on linguistic terms. The results are shown in Table 3 and aggregated fuzzy weight of respective machining characteristics is presented in Table 4. The average solution of machining response, A_b were calculated using the machining response given in Table 1 and Eq. (2). The $A_b$values each for MRR, machining depth, overcut and surface roughness were determined to be 5.537 mg/min, 43.962 µm, 14.464 µm and 0.161 µm, respectively. Positive and negative distances from average i.e., PDA and NDA values based on the criteria were determined using Eqs. (3) to (6), respectively, and presented in Tables 5 and 6. These values were used using Eqs. (7) and (9) to calculate the weighted sum of PDA and NDA of SP_a and SN_a, as given in Tables 7 and 8, respectively. The relative weight of each performance characteristics of MRR, machining depth, overcut and surface roughness were determined employing Eq. (8) as 0.068, 0.369, 0.247 and 0.316, respectively. Equations 10 and 11 were used to calculate NSP_a and NSN_a, using SP_a and SN_avalues, respectively. Appraisal score, AS_a were calculated normalizing NSP_a and NSN_avalues for each experimental run during process using Eq. (12).

Table 9 enlists values of SP_a, SN_a, NSP_a, NSN_a, AS_a and ranks each experimental run used in this experimental investigation. From this table, it is evident that experiment No. 12 of EMM process parametric combination has produced the highest AS_a value. Therefore, experiment No. 12 has the optimal process parametric setting during the micro-texturing of SS304 for the best multi-performance characteristics or desirable output responses among the nineteen experimental runs. However, to find an optimal process parametric combination, the average AS_a values for the respective level of input parameters based on experimental design were calculated by considering the average of various AS_a values at the same variable level for the respective column. The AS_a values for the respective parameters are shown in Table 10. Regardless of the type of micro-texturing characteristics, a higher AS_a value implies better performance.

Table 2. Linguistic variables described by triangular fuzzy numbers for the important weight of each performance parameters [20]

Importance	Abbreviation	Fuzzy weight
Lowest	L1	(0.0, 0.0, 0.1)
Lower	L2	(0.0, 0.1, 0.3)
Low	L3	(0.1, 0.3, 0.5)
Medium	M	(0.3, 0.5, 0.7)
High	H3	(0.5, 0.7, 0.9)
Higher	H2	(0.7, 0.9, 1.0)
Highest	H1	(0.9, 1.0, 1.0)

Table 3. Importance of machining responses

Machining Response	Decision Makers			
	DM1	DM2	DM3	DM4
MRR	L3	L2	L2	L1
Overcut	H1	H2	H3	H3
Machining Depth	H2	M	L3	M
Surface Roughness	H3	H3	M	H2

Table 4. Aggregated fuzzy weights of performance parameters

Machining Response	Fuzzy weight
MRR	(0.025, 0.125, 0.300)
Overcut	(0.650, 0.825, 0.950)
Machining Depth	(0.350, 0.550, 0.725)
Surface Roughness	(0.500, 0.700, 0.875)

Table 5. Positive distance from average (PDA)

Expt. No.	MRR	Machining Depth	Overcut	Surface Roughness
1	0.000	0.000	0.509	0.765
2	0.029	0.000	0.396	0.554
3	0.246	0.076	0.157	0.000
4	0.355	0.213	0.000	0.000
5	0.102	0.000	0.394	0.623
6	0.210	0.000	0.274	0.230
7	0.517	0.211	0.000	0.000
8	0.499	0.349	0.000	0.000
9	0.481	0.069	0.000	0.000
10	0.427	0.000	0.198	0.557
11	0.000	0.000	0.000	0.467
12	0.000	0.000	0.000	0.389
13	0.000	0.000	0.000	0.444
14	0.000	0.235	0.647	0.000
15	0.000	0.000	0.578	0.000
16	0.000	0.000	0.551	0.000
17	0.000	0.000	0.004	0.667
18	0.048	0.053	0.000	0.636
19	0.409	0.316	0.000	0.632

Table 6. Negative distance from average (NDA)

Expt. No.	MRR	Machining Depth	Overcut	Surface Roughness
1	0.133	0.360	0.000	0.000
2	0.000	0.063	0.000	0.000
3	0.000	0.000	0.000	0.031
4	0.000	0.000	0.950	0.534
5	0.000	0.163	0.000	0.000
6	0.000	0.040	0.000	0.000
7	0.000	0.000	0.507	0.540
8	0.000	0.000	0.784	0.664
9	0.000	0.000	0.611	0.540
10	0.000	0.112	0.000	0.000
11	0.422	0.284	0.210	0.000
12	0.476	0.178	0.231	0.000
13	0.801	0.142	0.120	0.000
14	0.711	0.000	0.000	2.266
15	0.440	0.026	0.000	1.366
16	0.314	0.108	0.000	0.025
17	0.025	0.048	0.000	0.000
18	0.000	0.000	0.044	0.000
19	0.000	0.000	0.251	0.000

Table 7. Weighted sum of PDA

MRR	Machining Depth	Overcut	Surface Roughness	SP_a
0.000	0.000	0.126	0.242	0.367
0.002	0.000	0.098	0.175	0.275
0.017	0.028	0.039	0.000	0.084
0.024	0.079	0.000	0.000	0.103
0.007	0.000	0.097	0.197	0.301
0.014	0.000	0.068	0.073	0.155
0.035	0.078	0.000	0.000	0.113
0.034	0.129	0.000	0.000	0.163
0.033	0.026	0.000	0.000	0.058
0.029	0.000	0.049	0.176	0.254
0.000	0.000	0.000	0.148	0.148
0.000	0.000	0.000	0.123	0.123
0.000	0.000	0.000	0.140	0.140
0.000	0.087	0.160	0.000	0.247
0.000	0.000	0.143	0.000	0.143
0.000	0.000	0.136	0.000	0.136
0.000	0.000	0.001	0.211	0.212
0.003	0.019	0.000	0.201	0.224
0.028	0.117	0.000	0.200	0.344

Table 8. Weighted Sum of NDA

MRR	Machining Depth	Overcut	Surface Roughness	SN_a
0.009	0.133	0.000	0.000	0.142
0.000	0.023	0.000	0.000	0.023
0.000	0.000	0.000	0.010	0.010
0.000	0.000	0.235	0.169	0.403
0.000	0.060	0.000	0.000	0.060
0.000	0.015	0.000	0.000	0.015
0.000	0.000	0.125	0.171	0.296
0.000	0.000	0.194	0.210	0.403
0.000	0.000	0.151	0.171	0.321
0.000	0.041	0.000	0.000	0.041
0.029	0.105	0.052	0.000	0.185
0.032	0.066	0.057	0.000	0.155
0.054	0.052	0.030	0.000	0.136
0.048	0.000	0.000	0.716	0.764
0.030	0.010	0.000	0.432	0.471
0.021	0.040	0.000	0.008	0.069
0.002	0.018	0.000	0.000	0.019
0.000	0.000	0.011	0.000	0.011
0.000	0.000	0.062	0.000	0.062

Thus, the optimal setting for micro-texturing process parametric combination resembles to the level having the highest AS_a value. Based on AS_avalues listed in Table 10, the optimum setting for electrochemical microtexturing process during micro-texturing of SS304 was obtained as 10 V voltage (level 2), 40% duty ratio (level 3), 5 kHz frequency (level 3), 100 µm IEG (level 1), 5 m^3/h flow rate (level 4) and machining time 5 min (level 4). The differences among the greater and the smaller values of the appraisal scores of process parameters have been found to be 0.483 for voltage, 0.241 for duty ratio, 0.450 for frequency, 0.062 for IEG, 0.316 for flow rate and 0.347 for machining time. In addition, the variations between larger and smaller AS_a values for various parameters at all four levels were compared to identify the most

effective factor influencing performance characteristics. The order of importance of the parameters for the multi-performance characteristics was determined by this assessment. The greatest value indicates the most influencing controllable factor. Hence, the maximum value of 0.483 corresponding to voltage, establishes the fact that the voltage has the highest influence on the multi-performance characteristics amongst all the electrochemical microtexturing process parameters. Based on this comparison, the sequence of parameters in this experimental investigation to the multi-performance characteristics in the micro-texturing process are voltage, frequency, machining time, flow rate, duty ratio and inter-electrode gap with their corresponding AS_a values of 0.483, 0.450, 0.347, 0.316, 0.241 and 0.062, respectively. To validate the optimal process parametric combination during micro-texturing of SS304, confirmation experiment was accomplished, and the performance characteristics are shown in Table 11. It is evident from this table that the micro-texturing performance characteristics during validation experiment are improved even when compared to experiment No. 12, which is ranked 1. Figure 10 shows the image of micro-textured surface after the confirmation experiment. This validates that optimal process parametric combination achieved through EDAS method produced the optimal machining characteristics and can be used successfully in multi-attribute decision making.

Table 9. Normalized values of SP_a, SN_a, NSP_a, NSN_a, calculation of AS_a and ranking of experimental runs

Expt.	SP_a	SN_a	NSP_a	NSN_a	AS_a	Rank
1	0.367	0.142	1.000	0.814	0.907	3
2	0.275	0.023	0.748	0.970	0.859	7
3	0.084	0.010	0.228	0.987	0.607	13
4	0.103	0.403	0.279	0.473	0.376	17
5	0.301	0.060	0.819	0.921	0.870	6
6	0.155	0.015	0.421	0.981	0.701	11
7	0.113	0.296	0.307	0.613	0.460	14
8	0.163	0.403	0.442	0.472	0.457	15
9	0.058	0.321	0.159	0.579	0.369	18
10	0.254	0.041	0.691	0.946	0.819	8
11	0.148	0.185	0.402	0.757	0.580	2
12	0.123	0.155	0.335	0.797	0.566	1
13	0.140	0.136	0.382	0.822	0.602	5
14	0.247	0.764	0.671	0.000	0.336	19
15	0.143	0.471	0.389	0.384	0.386	16
16	0.136	0.069	0.370	0.910	0.640	12
17	0.212	0.019	0.576	0.975	0.776	10
18	0.224	0.011	0.609	0.986	0.797	9
19	0.344	0.062	0.937	0.919	0.928	4

Table 10. Response table for AS_a at each level

Process Parameters	Average AS_a				Max- Min
	Level 1	Level 2	Level 3	Level 4	
Voltage	0.637	0.859	0.607	0.376	0.483
Duty ratio	0.625	0.625	0.701	0.460	0.241
Frequency	0.457	0.369	0.819	0.634	0.450
Inter Electrode Gap	0.628	0.580	0.566	0.602	0.062
Flow Rate	0.336	0.386	0.640	0.652	0.316
Machining Time	0.581	0.776	0.797	0.928	0.347

Table 11. Confirmation experimental result at optimal parametric setting

Voltage (V)	Duty ratio (%)	Frequency (kHz)	IEG (μm)	Flow Rate (m^3/h)	Machining Time (min)	MRR (mg/min)	Overcut (μm)	Depth (μm)	R_a (μm)
10	40	5	100	5	5	5.2	25.41	8.2	0.0278

At a specific parametric configuration of 10 V voltage,100 μm IEG, 5 kHz frequency, 5 m^3/h flow rate, 40% duty ratio and 5 min machining time, the micro-textured picture of the micro circular pattern is generated as shown in Figure 10 after confirmation experiment. Due to regulated anodic dissolution, the micro scale pattern is homogeneous throughout the micromachining region. Due to reduced stray current effect, the dimensional accuracy is higher. Due to

uniform dissolution, the depth is approximately equal in the pattern. As a result of regulated etching, the surface finish is also fine. From the confirmation experiment, the best surface characteristics are achieved than other experimental results.

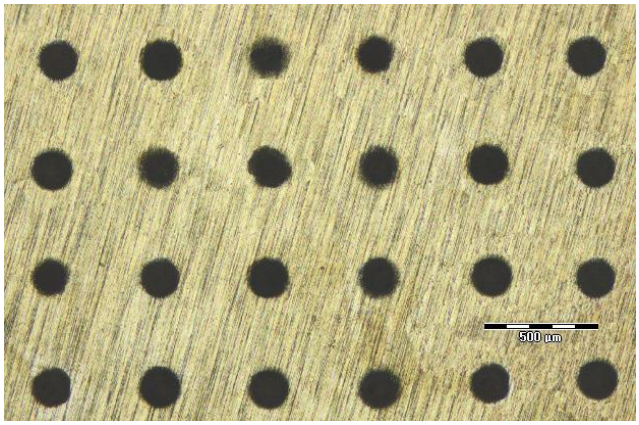

Figure 10. Regular micro circular pattern after confirmation experiment

The 3D image of the micro circular impression is shown in Figure 11. The two dimensional (2D) depth profile with a magnitude of 24.1 µm is depicted in Figure 12, and the 2D roughness profile of this circular impression with a value of 0.0526 µm is represented in Figure 13. These three profiles are captured by three dimensional profilometer from regular micro circular pattern.

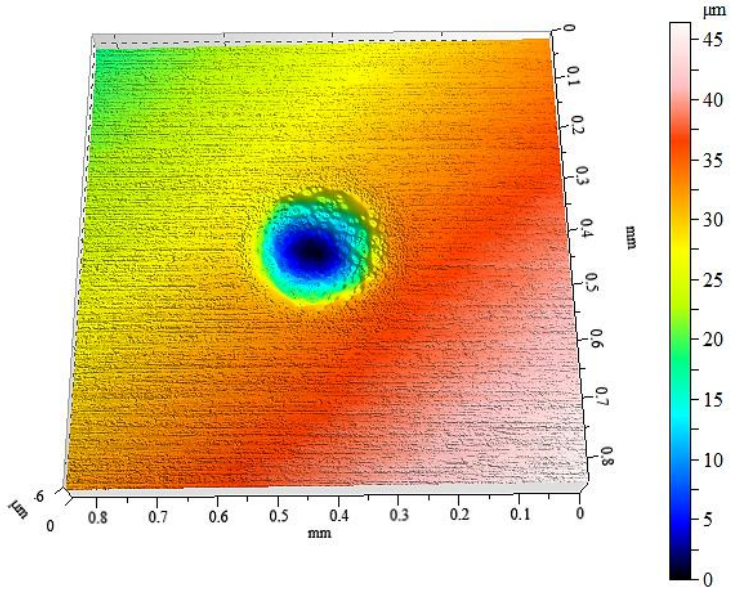

Figure 11. 3D profile of micro circular impression

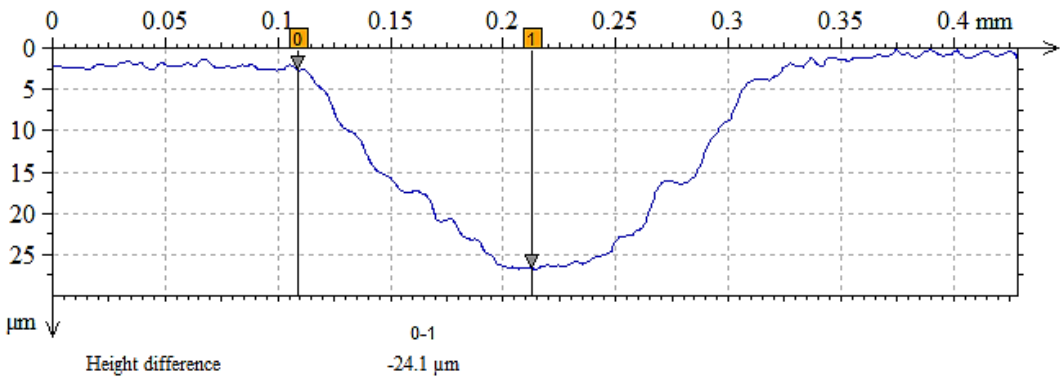

Figure 12. 2D depth profile

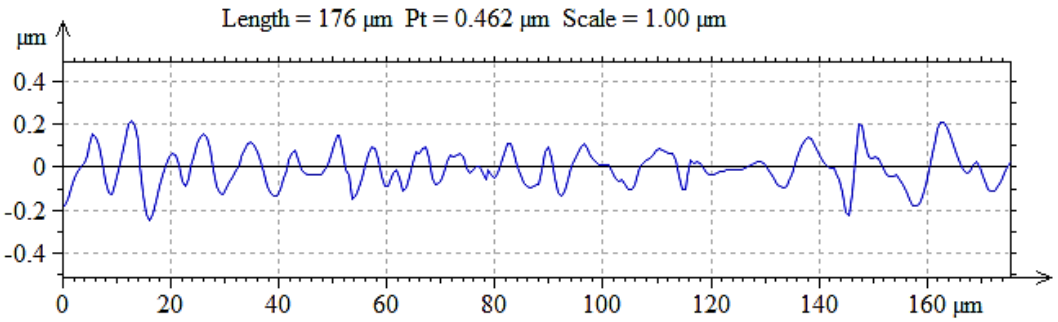

Figure 13. Surface roughness profile

Figure 14 shows a 3D image and 2D roughness profile of segment of micro circular impression with a value of 190.94 nm acquired by the Atomic Force Microscope (Nanosurf Easy Scan 2, Switzerland).

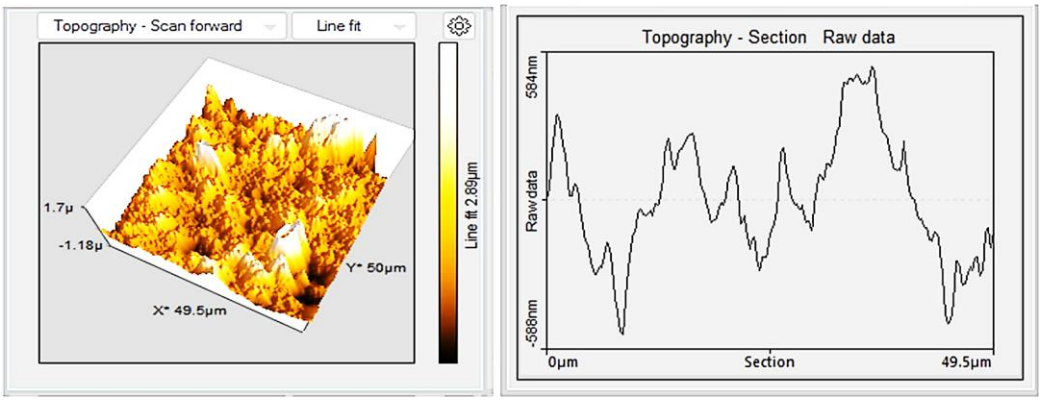

Figure 14. 3D segment with 2D roughness profile

4. CONCLUSIONS

A substitute concept of electrochemical microtexturing is used for manufacturing micro scale patterns. The effect on micro textured characteristics of process variables is investigated and the EDAS method is used to obtain optimized parameters to achieve better micropatterns. It is possible to draw the following conclusions:

i) An efficient and effective concept of maskless electrochemical microtexturing is applied to carry out the investigation using indigenously fabricated investigational setup. One patterned tool can produce more than nineteen samples without distortion of mask.

ii) EDAS method combined with triangular fuzzy numbers for determination of aggregated fuzzy weight was used to determine the optimal process parametric combination to achieve higher MRR & machining depth and lower overcut & surface roughness from various parametric combinations used in the present experimental investigation.

iii) Voltage has the highest influence on the multi-performance characteristics amongst all the EMM process parameters. The sequence of influential parameters in this experimental investigation to the multi-performance characteristics in the microtexturing process are voltage, frequency, machining time, flow rate, duty ratio and IEG with their corresponding values 0.483, 0.450, 0.347, 0.316, 0.241 and 0.062, respectively.

iv) The optimal process parametric setting for electrochemical microtexturing process during micro-texturing of SS304 was obtained as 10 V voltage, 40% duty ratio, 5 kHz frequency, and 100 µm IEG, 5 m^3/h flow rate and machining time 5 min. In addition, the validation experiment using the obtained optimal parametric setting corroborated the novel strategy, method and framework used in the present experimental investigation to enhance the overall microtexturing process.

Furthermore, wide-ranging investigations may be carried out in development of intricate patterned tool design and texturing on curved surfaces for advanced engineering applications.

ACKNOWLEDGMENT

This study was not supported by any grants from funding bodies in the public, private, or not-for-profit sectors.

CONFLICT OF INTEREST

The authors declare that they have no conflicts of interest to report regarding the present study.

AUTHORS CONTRIBUTION

S. Kunar (Conceptualization; Methodology; Formal analysis; Validation; Data curation; Investigation; Writing; Resources)

AVAILABILITY OF DATA AND MATERIALS

The data supporting this study's findings are available on request from the corresponding author.

ETHICS STATEMENT

Not applicable.

REFERENCES

[1] X. M. Li, D. Reinhoudt, M. Crego-Calama, "What do we need for a superhydrophobic surface? A review on the recent progress in the preparation of superhydrophobic surfaces," *Chemical Society Reviews*, vol. 36, no. 8, pp. 1350-1368, 2007.

[2] E. Lamers, X. F. Walboomers, M. Domanski, J. Riet, F. C. M. J. M. van Delft, R. Luttge, et al., "The influence of nanoscale grooved substrates on osteoblast behaviour and extracellular matrix deposition," *Biomaterials*, vol. 31, pp. 3307–3316, 2010.

[3] A. Amanov, I. S. Cho, Y. S. Pyoun, C. S. Lee, I. G. Park, "Micro-dimpled surface by ultrasonic nanocrystal surface modification and its tribological effects," *Wear*, vol. 286-287, pp. 136–144, 2012.

[4] T. Burzynski, M. Papini, "Level set methods for the modeling of surface evolution in the abrasive jet micromachining of features used in MEMS and microfluidic devices," *Journal of Micromechanics and Microengineering*, vol. 20, no. 9, p. 085004, 2010.

[5] J. Zhang, Y. Meng, "A study of surface texturing of carbon steel by photochemical machining," *Journal of Materials Processing Technology*, vol. 212, no. 10, pp. 2133-2140, 2012.

[6] S. Kunar, B. Bhattacharyya, "Influence of various flow methods during fabrication of micro ellipse pattern by maskless electrochemical micromachining," *Journal of Manufacturing Processes*, vol. 35, pp. 700-714, 2018.

[7] A. G. Demir, B. Previtali, N. Lecis, "Development of laser dimpling strategies on TiN coatings for tribological applications with a highly energetic Q- switched fibre laser," *Optics & Laser Technology*, vol. 54, pp. 53-61, 2013.

[8] S. Kunar, B. Bhattacharyya, "Electrochemical microsurface texturing with reusable masked patterned tool," *Engineering Science and Technology, an International Journal*, vol. 21, no. 5, pp. 1095-1103, 2018.

[9] S. Kunar, B. Bhattacharyya, "Investigation on surface structuring generated by electrochemical micromachining," *Advances in Manufacturing*, vol. 5, no. 3, pp. 217– 230, 2017.

[10] K. L. Senthil Kumar, R. Sivasubramanian, K. Kalaiselvan, "Selection of optimum parameters in non-conventional machining of metal matrix composite," *Port Electrochimica Acta*, vol. 27, no. 4, pp. 477–486, 2009.

[11] A. Noorul Haq, P. Marimuthu, R. Jeyapaul, "Multi response optimization of machining parameters of drilling Al/SiC metal matrix composites using grey relational analysis and Taguchi method," *International Journal of Advanced Manufacturing Technology*, vol. 37, pp. 250-255, 2008.

[12] C. Zhao, P. Ming, X. Zhang, G. Qin, J. Shen, L. Yan, et al., "Through-mask electrochemical micromachining with reciprocating foamed cathode," *Micromachines*, vol. 11, no. 2, p. 188, 2020.

[13] M. Wang, Y. Shang, K. He, X. Xuefeng, C. Guoda, "Optimization of nozzle inclination and process parameters in air-shielding electrochemical micromachining," *Micromachines*, vol. 10, p. 846, 2019.

[14] N. Lusi, D. R. Pamuji, A. Afandi, G. S. Prayogo, "Optimization design of electrochemical machining process of SKD11 tool steel using weighted principal component analysis (WPCA)," in *IOP Conference Series: Materials Science and Engineering*, vol. 854, p. 012024, 2020.

[15] D. S. Patel, V. Agrawal, J. Ramkumar, V. K. Jain, G. Singh, "Micro-texturing on free-form surfaces using flexible-electrode through-mask electrochemical micromachining," *Journal of Materials Processing Technology*, vol. 282, p. 116644, 2020.

[16] J. N. Krishnan, J. Deepak, P. Hariharan, "Multi-response optimization of electrochemical micromachining on masked SS304," *Engineering Research Express*, vol. 2, no. 1, p. 015041, 2020.

[17] R. Thanigaivelan, R. Arunachalam, "Optimization of process parameters on machining rate and overcut in electrochemical micromachining using grey relation analysis," *Journal of Scientific & Industrial Research*, vol. 72, pp. 36-42, 2013.

[18] B. Juodagalvienė, Z. Turskis, J. Šaparauskas, A. Endriukaitytė, "Integrated multi-criteria evaluation of house's plan shape based on the EDAS and SWARA methods," *Engineering Structures and Technologies*, vol. 9, pp. 117-125, 2017.

[19] M. K. Ghorabaee, E. K. Zavadskas, L. Olfat, Z. Turskis, "Multi-criteria inventory classification using a new method of evaluation based on distance from average solution (EDAS)," *Informatica*, vol. 26, pp. 435-451, 2015.

[20] D. Zindani, S. R. Maity, S. Bhowmik, "Fuzzy-EDAS (Evaluation based on distance from average solution) for material selection problems," in *Lecture Notes on Multidisciplinary Industrial Engineering*, pp. 755-771, 2019.

[21] A. P. Tiwary, B. B. Pradhan, B. Bhattacharyya, "Application of multi-criteria decision-making methods for selection of micro-EDM process parameters," *Advances in Manufacturing*, vol. 2, pp. 251-258, 2014.